Chemical Engineering Journal 155 (2009) 199–206

Contents lists available at ScienceDirect

Chemical Engineering Journal

journal homepage: www.elsevier.com/locate/cej

Biosorption of chromium (III) by orange (*Citrus cinensis*) waste: Batch and continuous studies

A.B. Pérez Marín, M.I. Aguilar*, V.F. Meseguer, J.F. Ortuño, J. Sáez, M. Lloréns

Department of Chemical Engineering, University of Murcia, 30071 Murcia, Spain

ARTICLE INFO

Article history:
Received 24 March 2009
Received in revised form 15 July 2009
Accepted 16 July 2009

Keywords:
Orange waste
Biosorption
Chromium
Fixed-bed
Continuous
Breakthrough curves

ABSTRACT

The present study explores the ability of orange waste biomass to remove Cr (III) from aqueous solutions. Batch kinetic and isotherm studies were carried out on a laboratory scale to evaluate the adsorption capacity of orange waste. The effects of particle size, adsorbent dose and solution pH on Cr (III) removal were also studied. The results showed that the higher the adsorbent dosage and the pH, the higher the percentage of metal removal. No significant influence of particle size on sorption capacity was observed in the experimental conditions studied. A kinetic study revealed that the adsorption of Cr (III) onto orange waste was a gradual process and equilibrium was reached within 3 days. A pseudo-second order model was the most appropriate to describe the kinetic experimental data. Equilibrium assays displayed a maximum sorption capacity ranging from 0.57 mmol/g to 1.44 mmol/g when the pH increased from 3 to 5, according to the Sips model, which along with the Redlich–Peterson equation, is very suitable for correlating equilibrium data. The use of the studied adsorbent in the removal of chromium in continuous mode was successful and the breakthrough curves were adequately represented by BDST model. Due to the slow kinetics of chromium sorption onto orange waste, the sorption capacity in batch assays was higher than that in continuous assays.

1. Introduction

Industrialization has led to increased amounts of heavy metals being dumped into the environment [1]. These kinds of substances are stable and persistent environmental contaminants since they cannot be degraded or destroyed, and therefore tend to accumulate in the soils, seawater, freshwater and sediments. Heavy metals are known to have adverse effects on the environment and human health. For example, excessive levels of metals in the marine environment can affect marine biota and pose a risk to human consumers of seafood.

Chromium is used in a wide variety of industrial applications, including steel production, electro-plating, leather tanning, nuclear power production, textile manufacturing, wood preservation, the anodising of aluminium, water-cooling and chromate preparation [2,3]. Long time contact with chromium causes skin allergy and cancer [4]. In water chromium (III) is toxic to fish when its concentration exceeds 5.0 mg/L [5,6]. The maximum allowable levels of Cr in drinking water considered safe by the US Environmental Protection Agency is 0.1 mg/L, although the World Health Organisation sets the upper limit at 0.01 mg/L.

The elimination of chromium from wastewaters is therefore a priority concern. Many physico-chemical methods have been developed for heavy metal removal from aqueous solutions, including precipitation, oxidation–reduction, ionic exchange, filtration, electrochemical treatment, membrane techniques and recovery by evaporation. However, all these methods involve high operating costs and may produce large volumes of solid wastes [7,8]. Recently, the search for an effective, simple and cheap treatment for the removal of heavy metals has turned its attention on biosorption, using materials of biological origin. Indeed, several materials have demonstrated their capacity to retain chromium, including carrot residues [9], eggshells [10], coir pitch [11], rice hull ash [12] and olive stone [13].

To effectively apply these materials to the removal of heavy metals, it is essential to understand the mechanism of interaction between the metal ions and the sorbent material, as well as the parameters that affect metal biosorption. In this study, a waste from the orange juice industry was evaluated for its ability to remove Cr (III) from aqueous solutions through sorption. The influence of parameters, such as adsorbent dosage, particle size and pH in the solution, on the biosorption process was examined. Various kinetic and isotherm parameters were also evaluated from batch biosorption assays. Since, in industrial processes, continuous reactors are preferred, column breakthrough data were obtained and analysed using the BDST model.

* Corresponding author. Tel.: +34 868 88 70 91; fax: +34 868 88 41 48.
E-mail address: maguilar@um.es (M.I. Aguilar).

1385-8947/$ – see front matter © 2009 Elsevier B.V. All rights reserved.
doi:10.1016/j.cej.2009.07.034

2. Materials and methods

2.1. Adsorbent

The orange waste used as adsorbent in this study was provided by Agrumexport, S.L., an orange juice manufacturing company located in Murcia (Spain). The orange waste was first cut into small pieces, extensively washed with tap water to remove adhering dirt and soluble components such as tannins, resins, reducing sugar and colouring agents, and then oven-dried at 50–60 °C until constant weight. The washed and dried material was crushed and sieved to obtain a particle size lower than 1.5 mm. Biomass was characterized by Fourier transform infrared spectroscopy (FTIR). The spectra of the biosorbent before and after metal ion binding were recorded in a Fourier transform infrared spectrophotometer (Perkin Elmer 16F PC) with the samples prepared as KBr discs.

2.2. Chemical

Stock metal solutions (2000 mg/L) were prepared by dissolving 15.39 g of $Cr(NO_3)_3{\cdot}9H_2O$ supplied by Panreac in a mixture of 100 mL of distilled water and 10 mL of concentrated nitric acid, and diluting to 1 L with distilled water. All working solutions were prepared by diluting the stock solution with distilled water to the needed concentration. All chemicals used were of analytical reagent grade and were purchased from Panreac.

2.3. Experimental procedure

2.3.1. Batch experiments

Experiments were performed to determine the effect of various parameters (adsorbent concentration, particle size and pH) on the sorption of Cr^{3+} onto orange waste. These studies were carried out in batch mode and at constant room temperature. Accurately weighed amounts of biomass were added to glass flasks containing 50 mL of metal solution at a concentration of 100 mg/L. The mixtures were stirred magnetically and their pH was continuously adjusted to the desired value using small volumes of HNO_3 or NH_4OH dilute solutions. After 3 days, which is more than sufficient to reach equilibrium, samples were filtered through glass fiber prefilters (Millipore AP40) and the filtrates were analysed for residual metal ion concentration by atomic absorption spectrophotometry (Perkin Elmer model AA300) with an air-acetylene flame.

In order to study the effect of particle size on Cr^{3+} sorption, experiments were carried out at pH = 4 with 0.2 g of biomass of different particle sizes (<0.15 mm, 0.15–0.3 mm, 0.3–0.5 mm, 0.5–0.8 mm, 0.8–1 mm, 1–1.25 mm, 1.25–1.5 mm, 1.5–2.5 mm, <1.5 mm).

The effect of adsorbent concentration on sorption of Cr^{3+} was obtained by adding 0.0125 g, 0.025 g, 0.05 g, 0.075 g, 0.1 g, 0.15 g, 0.2 g, 0.25 g, 0.3 g, 0.35 g or 0.4 g of adsorbent (particle size fraction <1.5 mm) to glass flasks containing the metal solution.

To investigate the effect of pH on the biosorption of Cr^{3+}, the pH of solutions were adjusted to 2, 3, 4 and 5 (adsorbent dosage = 4 g/L, particle size fraction <1.5 mm).

Isotherm assays were carried out at three different pH values (3, 4 and 5) by varying the initial concentration of metal from 0 mg/L to 300 mg/L (adsorbent dosage = 4 g/L, particle size fraction <1.5 mm).

Kinetic studies were carried out in a glass beaker with magnetic stirring at room temperature (25 °C), adding 4 g of biomass was added to 1 L of metal solution (100 mg/L) and keeping the pH of the suspension constant throughout the experiment. The assays were carried out at three different pH values (3, 4 and 5). Samples ($\approx$5 cm^3) were withdrawn at suitable time intervals using 20 cm^3 syringes, filtered immediately through glass fiber prefilters and then analysed for metal ion concentration using an atomic absorption spectrophotometer.

Metal uptake at different adsorbent-solution contact times (q, mmol/g) was calculated using the general definition:

$$q = \frac{C_0 \cdot V_0 - C_t \cdot V_t}{m} \quad (1)$$

where C_0 and C_t are the metal concentrations in solution (mmol/L) at time 0 and t, respectively, V_0 and V_t are the solution volumes (L) at time 0 and t, respectively, and m is the mass of the biosorbent used (g). After reaching equilibrium, Eq. (1) was used to calculate the adsorption capacity of the adsorbent, q_e, using C_t and V_t at equilibrium.

2.3.2. Continuous experiments

The continuous sorption experiments were carried out in an acrylic tubular column, 50 cm high and 2.2 cm internal diameter. The orange waste (particle size from 0.6 mm to 1.5 mm) was packed in the column between glass beads, which prevents the orange waste from washing out and enables a uniform inlet flow into the column. Two different bed heights (25.5 cm and 34 cm) were tested. These bed heights correspond to 18 g and 24 g of orange waste, respectively. A 20 mg/L Cr^{3+} solution at pH 4 was pumped upwards by a peristaltic pump, at 8.5 mL/min, to the column reactor. The solution was fed from the bottom of the reactor and samples were collected at the top of the column during the time-course of the experiments. Column effluent samples were collected regularly by a programmable fraction collector and analysed by atomic absorption spectrometry (Perkin Elmer model AA300). The pH of the effluent samples was also measured. Each experiment was carried out until the effluent Cr^{3+} concentration (C_t) were close to the influent concentration (C_0), $C_t/C_0 \cong 0.99$.

All batch and continuous experiments were performed in duplicate at least and the mean values are presented with a maximum deviation of 5% in all the studied cases. Blank samples were run under similar experimental conditions but in the absence of adsorbent. No chemical precipitation or losses of metal ions to the material employed were detected.

2.3.3. Modelling of kinetic, isotherm and breakthrough curves

Different theoretical models (Table 1) and mathematical treatments were applied to experimental data in order to find a model which adequately predicts breakthrough curves, kinetic and isotherm data. The models were fitted using the non-linear fitting facilities of the Solver add-in of Microsoft Excel. The validity of models was evaluated by the determination coefficient (r) and the average relative error function (ARE, %). This error function measures the relative differences between experimental values and those predicted by the models.

3. Results and discussion

3.1. FTIR analysis

In order to determine which functional groups are responsible for metal uptake, FTIR spectra of the biosorbent, before and after Cr^{3+} uptake, were recorded. The spectra of adsorbent were measured in the range of 400–4000 cm^{-1}. As can be seen in Fig. 1, the spectra show a number of absorption peaks, indicating the complex nature of the material studied.

The FTIR spectrum of orange waste exhibits a broad peak at 3422 cm^{-1}, which corresponds to the O–H stretching vibrations of cellulose, pectin, absorbed water, hemicellulose, and lignin [14]. The OH stretching vibrations occur within a broad range of frequencies, indicating the presence of free hydroxyl groups and bonded OH bands of carboxylic acids [15,16]. The band at 2924 cm^{-1} indicates

Table 1
Kinetic, isotherm and continuous fixed bed models used in the work.

	Parameters
Kinetic models	
Pseudo-first order $q_t = q_e \cdot (1 - e^{-k_1 \cdot t})$	q_e, equilibrium sorption capacity (mmol/g) k_1, pseudo-first order rate constant (min^{-1})
Pseudo-second order $q_t = \frac{t}{(1/(k_2 \cdot q_e^2)) + (t/q_e)}$	q_e, equilibrium sorption capacity (mmol/g) k_2, pseudo-second order rate constant (g/mmol min)
Elovich equation $q_t = \frac{1}{\beta} \cdot \ln(\alpha \cdot \beta) + \frac{1}{\beta} \cdot \ln\ t$	α, constant in Elovich equation (mmol/g min) β, exponent in Elovich equation (g/mmol)
Intraparticle diffusion $q_t = k \cdot \sqrt{t}$	k, intraparticle diffusion rate constant ($mmol/g\ min^{1/2}$)
Isotherm models	
Langmuir $q_e = \frac{q_{max} \cdot b \cdot C_e}{1 + b \cdot C_e}$	q_{max}, maximum sorption capacity (mmol/g) b, Langmuir constant (L/mmol)
Freundlich $q_e = k_F \cdot C_e^{1/n}$	k_F, Freundlich constant $(L/g)^{-1/n}$ n, Freundlich exponent
Sips $q_e = \frac{q'_{max} \cdot b' \cdot C_e^{1/n'}}{1 + b' \cdot C_e^{1/n'}}$	q'_{max}, maximum sorption capacity (mmol/g) b', Sips constant $(L/mmol)^{-1/n'}$ n' Sips exponent
Redlich–Peterson $q_e = \frac{k_R \cdot C_e}{1 + a_R \cdot C_e^{\beta}}$	k_R, Redlich–Peterson constant (L/g) a_R, Redlich–Peterson constant $(L/mg)^{\beta}$ β, Redlich–Peterson exponent
Continuous fixed-bed model	
BDST $\frac{C}{C_0} = \frac{1}{1 + \exp(((N_0 \cdot K_a \cdot H)/v) - K_a \cdot C_0 \cdot t)}$	N_0, volumetric sorption capacity (mmol/g) K_a, kinetic constant (L/mmol min)

symmetric or asymmetric CH stretching vibration of aliphatic acids. The peak at 2854 cm^{-1} was the symmetric stretching vibration of CH_2 due to CH bonds of aliphatic acids. Bands around 1647 cm^{-1} and 1736 cm^{-1} are indicative of the existence of free and esterified carboxyl groups, respectively [17]. The peak at 1373 cm^{-1} may be assigned to symmetric stretching of $-COO^-$. The bands observed at 1027–1039 cm^{-1} were assigned to C–O stretching of alcohols and carboxylic acids [18]. Similar FTIR spectra were obtained by Lodeiro et al. [19] with orange peel. When the biomass was loaded with chromium, differences in the positions of the absorbance peaks appeared. Band shifting and possible involvement of hydroxyl groups were observed around the broad peak at 3422 cm^{-1} in the sorption process. In the spectrum of the chromium-loaded biomass, there was a decrease in peak intensity at 2854 cm^{-1} due to the interaction between chromium ions and different C–H groups in the biomass. No change was observed in the free carboxyl band at 1736 cm^{-1}, but the shift of the asymmetric and symmetric C=O bands (1647–1636 cm^{-1}) indicates a degree of carboxyl bonding. Besides, Cr^{3+} sorption result in a relative decrease in free carboxyl

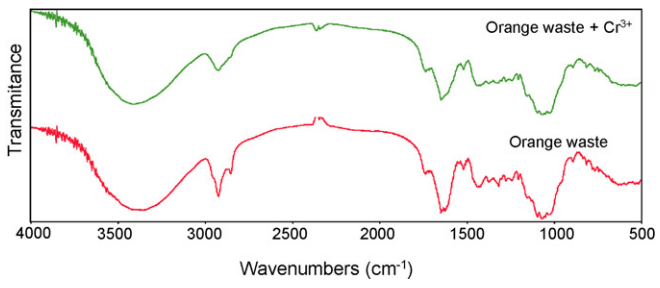

Fig. 1. FTIR spectra of the orange waste in BrK disk, before and after adsorption of Cr (III).

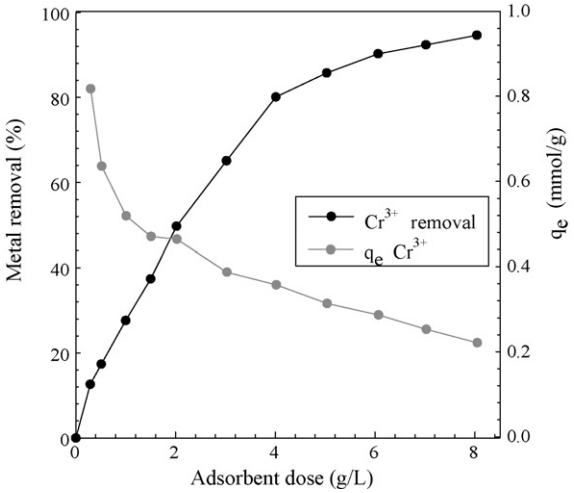

Fig. 2. Effect of orange waste concentration on chromium removal. Particle size <1.5 mm; $[Cr^{3+}]_0$ = 100 mg/L, pH = 4 and contact time = 3 days.

band intensity (1636 cm^{-1}) in relation to esterified carboxyl band intensity (1736 cm^{-1}). From these spectra it seems that carboxyl and hydroxyl groups are the main functional groups involved in Cr^{3+} bonding to the orange waste. The importance of these groups has been demonstrated in assays carried out with this biomass with the mentioned functional groups blocked [20].

3.2. Batch biosorption experiments

3.2.1. Effect of adsorbent dose on Cr^{3+} uptake

The effect of adsorbent dose on Cr^{3+} uptake by orange waste is illustrated in Fig. 2. In view of the obtained results, it can be concluded that the adsorbent dose strongly affects metal removal. The increase in adsorbent concentration up to 4 g/L resulted in a large increase in the percentage of metal uptake (0–80% metal uptake). The increase in the percentage of metallic ion removed with increasing biosorbent doses could be attributed to increased adsorbent surface area, which could increase the number of adsorption sites available. Any further increase in adsorbent concentration did not significantly affect the percentage of metal removal, perhaps because almost all the ions had been bound to the sorbent and to the establishment of equilibrium between the ions bound to the solid phase and those remaining in solution. On the contrary, a decrease in sorption capacity (q_e) was observed when the biosorbent dose was further increased, which can be explained by initial concentration gradient between the solid adsorbent and the bulk liquid [21]. Taking into account the Cr^{3+} percentage removal and the Cr^{3+} uptake (mmol/g), an adsorbent dose of 4 g/L was selected for all further experiments.

3.2.2. Effect of particle size on Cr^{3+} uptake

Fig. 3 shows the effect of particle size on Cr^{3+} sorption by orange waste. No significant differences were observed in the sorption capacity of the individual fractions with a particle size lower than 1.5 mm. In porous materials, the contribution of external surface area to the total surface area is very limited. And so, particle size reduction has a negligible effect on increasing total surface area [22] and little effect on the adsorption capacity. Besides, in this kind of material, metal removal may be controlled by ionic exchange and so be independent of the accessible surface area. The material employed as biosorbent in this study presents a high porosity and also high quantities of light metals (Ca^{2+}, Mg^{2+}, Na^+, K^+), which are susceptible to being exchanged. The sorption capacity of a whole sample, particle size <1.5 mm, showed similar values of sorption

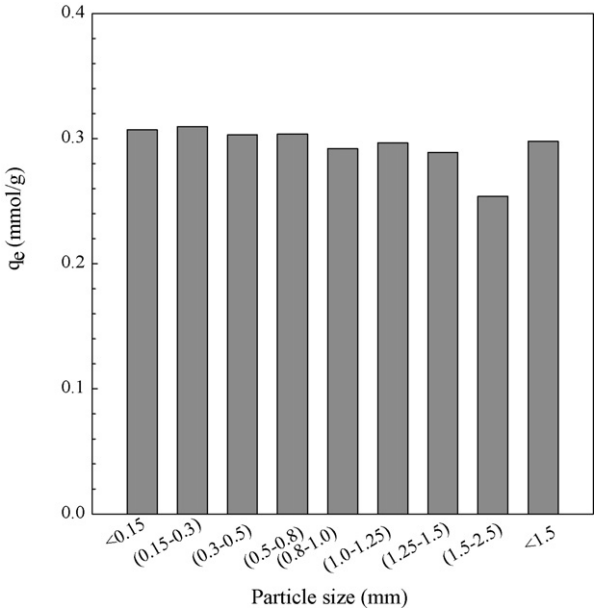

Fig. 3. Effect of particle size on chromium removal. [Adsorbent] = 4 g/L; $[Cr^{3+}]_0$ = 100 mg/L, pH = 4 and contact time = 3 days.

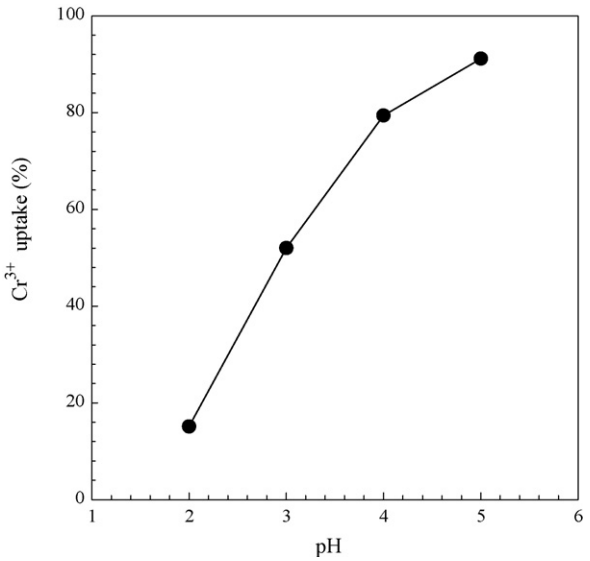

Fig. 4. Influence of pH on Cr^{3+} removal. [Adsorbent] = 4 g/L; particle size <1.5 mm; $[Cr^{3+}]_0$ = 100 mg/L and contact time = 3 days.

capacity to those of the individual fractions. Therefore, this whole fraction was selected for further test since the reduction and classification by size is facilitated.

3.2.3. Effect of pH

The pH value has been suggested as one of the major parameters controlling the sorption of metals with biosorbents [23–25]. The effect of pH on the removal of Cr^{3+} from aqueous solutions is shown in Fig. 4. As can be seen, the sorption capacity was clearly affected by this parameter, the amount of metal removed increasing with increasing pH. It is known that variations in pH could change the characteristics and availability of metal ions in solution as well as the chemical status of the functional groups responsible for biosorption [26].

At pH values above 3, other ionic species besides free Cr^{3+} may exist in solution, such as $Cr(OH)_2^+$, $Cr(OH)^{2+}$, $Cr_2(OH)_2^{4+}$ and $Cr_3(OH)_4^{5+}$ [27,28] and the biosorbent could present higher affinity for any of these species than for the free Cr^{3+} ion. Accordingly, the increase in sorption capacity with pH could be due to chromium speciation as well as to the degree of ionization of the active groups of the biomass.

The low adsorption capacity at low pH values can be explained by the competition of chromium with protons for the adsorption sites and by the electrostatic repulsion between protonated biomass surface and metal cations, since in this pH range chromium ions are present as cations [29,30]. At higher pH values, the lower number of H^+ and the greater number of surface ligands with negative charges resulted in greater metal adsorption. As mentioned above, carboxylic groups (–COOH) are important functional groups for metal uptake by orange waste. At pH values higher than 3–4, these groups are deprotonated and negatively charged and, consequently, the attraction of positively charged metal ions would be enhanced [31].

3.2.4. Sorption kinetics data

When designing a sorption processing system, it is desirable to know the rate at which the metal uptake will occur, since the required contact time will influence the physical size of the adsorber. Bearing this in mind, chromium sorption kinetics were obtained at three different pH values (3, 4, and 5), while the other experimental variables were kept constant. Fig. 5 shows the sorption kinetics of chromium on the orange waste at different pH values, as well as the fit to the kinetic models described in Section 2 (Table 1).

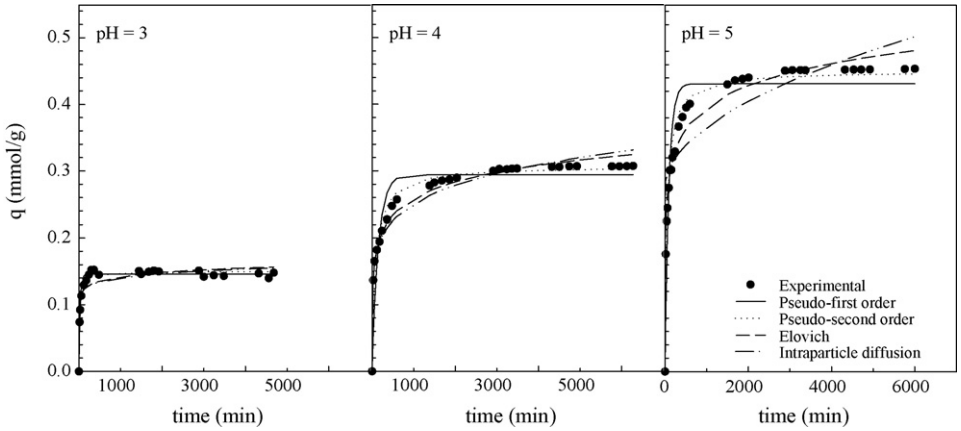

Fig. 5. Sorption kinetics of chromium onto orange waste. [Adsorbent] = 4 g/L; particle size <1.5 mm and $[Cr^{3+}]_0$ = 100 mg/L.

Table 2
Characteristic parameters of the different kinetic models and values of average relative errors (ARE, %) and coefficients of determination (r).

	Cr^{3+}		
	pH = 3	pH = 4	pH = 5
Pseudo-first order			
q_e (mmol/g)	0.146	0.294	0.449
k_1 (min^{-1})	0.033	0.007	0.011
ARE (%)	3.82	11.69	8.85
r	0.95	0.85	0.87
Pseudo-second order			
q_e (mmol/g)	0.149	0.307	0.457
k_2 (g/mmol min)	0.394	0.037	0.042
ARE (%)	2.55	7.71	4.20
r	0.97	0.95	0.97
Elovich			
α (mmol/g min)	4.94	0.047	0.143
β (mmol/g)	92.76	27.79	19.99
ARE (%)	7.84	1.47	5.00
r	0.77	0.98	0.97
Intraparticle diffusion			
k_i (mmol/g $min^{1/2}$)	0.003	0.005	0.008
ARE (%)	41.51	28.92	39.39
r	0	0	0

As can be seen, the sorption rate was quite fast at the initial stage being it gradually slowed down. The faster initial rate may be due to the availability of the uncovered sorption sites of the adsorbent at the beginning. Although more than 90% of the amount of chromium sorbed at equilibrium was reached in 3 h for pH = 3 and in 1 day for pH 4 and 5, chromium took almost 3 days to reach the equilibrium. As expected (Fig. 4), it was found that equilibrium biosorption capacities are significantly affected by solution pH, with higher pH favouring metal-ion removal.

As mentioned above, the experimental kinetic data were evaluated using several kinetic models: pseudo-first order, pseudo-second order, Elovich and intraparticle diffusion equations. The values of the characteristic parameters of the models, the determination coefficients and the values of the average relative error (ARE) are tabulated in Table 2.

The pseudo-first order equation did not provide an accurate fit to the experimental data (Fig. 5 and Table 2). The calculated values of q_e were lower than the experimental values. For most of the papers found in the bibliography whose data have been modelled using this equation, a good fit between experimental and theoretical model data were obtained in the early stages of sorption. Nevertheless, after approximately 40% metal ion uptake the correlation falls off rapidly and, therefore, the pseudo-first order kinetic model is not applicable to the whole sorption period [32]. In fact, the pseudo-first order approach assumes that the uptake rate is limited by only one process or mechanism acting on a single class of sorbing sites. So, this model does not seem to be appropriate for a heterogeneous surface such as that described in this study, since multiple sorption sites and mass transfer effects may exist.

The pseudo-second order model is based on the assumption that the rate-limiting step may be a chemical sorption involving valence forces through the sharing or exchange of electrons between adsorbent and adsorbate [33,34]. Contrary to the pseudo-first order equation, this model adequately predicts the sorption behaviour over the whole sorption period. It provides the smallest average relative error and the highest r for two of the three cases studied. In the other case, kinetics at pH = 4, the Elovich equation provides the best description of the system, the average relative error being lower than 8% and $r > 0.95$, and so this model could be considered acceptable to represent the kinetic data. Moreover, the equilibrium adsorption capacities, q_e, obtained with this model are more reasonable than those obtained with the pseudo-first order model when comparing predicted results with experimental data. According to the pseudo-second order model, k_2 is related to the rate of sorption. The data obtained confirm that the rate at pH = 3 is considerable higher than those obtained at higher pH values.

The Elovich equation assumes that the solid surface active sites are heterogeneous in nature and therefore, exhibit different activation energies for chemisorption [32]. The equation has previously been applied successfully to the sorption of heavy metal onto different biomass [35–37]. An Elovich plot gives curved lines or sharp changes in the gradient, the latter of which could be interpreted as a change in the adsorption mechanism. α is related to the rate of sorption, confirming that the sorption rate at pH = 3 is considerably higher than those obtained at higher pH values. In constrast, it was observed that the constant β decreases as the pH values increase. So, by increasing the pH value, within the range studied, the available adsorption surface of orange waste decreases. This model provide an adequate description of the kinetic data at pH values higher than 3 (ARE < 5%, $r > 0.97$).

The intraparticle diffusion equation did not provide a suitable fitting to the experimental data, giving values for the average relative error of more than 28%, for all the studied cases. This result indicates that intraparticle diffusion is not the rate controlling mechanism.

As a brief analysis of the kinetic data, it can be concluded that pseudo-second order kinetic model provides an accurate description of sorption kinetic onto orange waste for the studied cases. It is assumed, therefore, that the controlling mechanism of sorption is the chemical reaction.

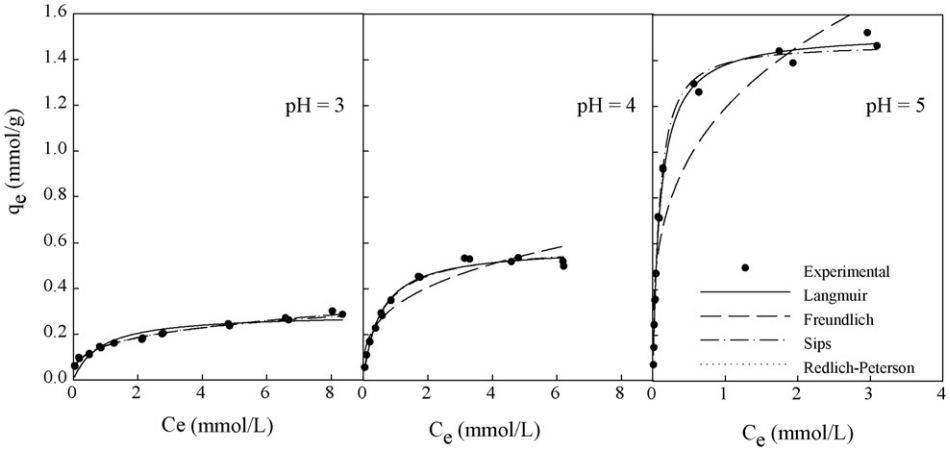

Fig. 6. Sorption isotherm of chromium onto orange waste. [Adsorbent] = 4 g/L; particle size <1.5 mm and contact time = 3 days.

Table 3
Characteristic parameters of the different isotherm models and values of average relative errors (ARE, %) and coefficients of determination (r).

	Cr^{3+}		
	pH = 3	pH = 4	pH = 5
Langmuir			
q_{max} (mmol/g)	0.241	0.776	1.52
b (L/mmol)	2.08	11.45	9.68
ARE (%)	11.05	8.46	12.2
r	0.960	0.994	0.996
Freundlich			
k_F $(L/g)^{1/n}$	0.147	0.640	1.19
n	3.94	3.36	3.39
ARE (%)	3.68	19.9	47.2
r	0.995	0.980	0.944
Sips			
q'_{max} (mmol/g)	0.559	0.855	1.52
b' $(L/mmol)^{1/n'}$	0.37	4.70	9.68
n'	2.76	1.32	1.00
ARE (%)	2.63	5.16	12.2
r	0.996	0.997	0.996
Redlich–Peterson			
k_R (L/g)	7.52	13.2	14.8
a_R $(L/mmol)^{\beta}$	49.5	18.1	9.7
β	0.77	0.89	1.0
ARE (%)	3.02	3.32	12.2
r	0.996	0.999	0.996

3.2.5. Sorption equilibrium data

Adsorption isotherms are basic requirements for designing any adsorption system. An accurate mathematical description of the equilibrium adsorption capacity is indispensable for reliable prediction of the adsorption parameters and quantitative comparison of adsorption behaviour for different biosorbent systems [38]. Fig. 6 shows the sorption isotherm of Cr (III) onto the orange waste at different pH values, as well as the fit to the isotherm models described in Section 2 (Table 1). For all isotherms, the amount of metal sorbed increases initially with the metal concentration at equilibrium but then reaches saturation. Once more, it can be corroborated that the sorption uptake is strongly affected by pH. The parameters of the isotherm models, the determination coefficients and the values of the average relative error (ARE) are shown in Table 3.

The Freundlich isotherm is an empirical equation used to describe multilayer adsorption with interaction between adsorbed ions [39]. This model predicts that the metal concentration on the adsorbent will increase as long as there is an increase in the metal concentration in the liquid phase. However, the experimental data indicate that an isotherm plateau is reached at a limiting value of the solid phase concentration. This plateau is not predicted by the Freundlich equation. Thus, in all the cases where there is evidence of this plateau (pH > 3), a great difference between the experimental equilibrium data and the predicted ones (ARE > 20%) were found.

The Langmuir model provides an adequate correlation of equilibrium data (ARE < 13%, r > 0.96). This model served to estimate the maximum metal uptake values where they could not be obtained experimentally. The constant b represents the affinity between the sorbent and sorbate. High values of b are reflected in the steep initial slope of a sorption isotherm, indicating desirable high affinity. Thus, high q_{max} and a steep initial isotherm slope (high b) are desirable. Comparing maximum sorption capacity of orange waste with those obtained with other adsorbents in assays carried out under similar conditions (0.22 mmol/g for coir pitch [11], 0.87 mmol/g for carrot residues [9], 1.30 mmol/g for rose waste biomass [40]), it can be concluded that orange waste has high adsorption capacity and can be considered a promising material for use as adsorbent.

The Sips isotherm effectively reduces to the Freundlich isotherm at low sorbate concentration, whereas it predicts a monolayer sorption capacity, characteristic of the Langmuir isotherm, at high sorbate concentrations. In the two cases in which the Langmuir model provides the best description of the experimental data (pH = 4 and 5), the values of the exponent n were closest to 1. Similar to the Sips model constants, the same trend was observed for the Redlich–Peterson model constants. The exponent β values were close to 1 at pH > 3. The models involving three fitting parameters provided better correlation of the equilibrium data (ARE < 13%, r > 0.99) than the two-parameter models.

3.3. Continuous biosorption experiments

Batch biosorption assays give fundamental information related with the chromium biosorption performance of a given biosorbent. However, in most industrial wastewater treatment units, a continuous mode of operation is preferred. Therefore, continuous biosorption experiments were also carried out. The performance of the column bed is usually described through the concept of a breakthrough curve, which is obtained by plotting the measured concentration divided by the inlet concentration (C/C_0) against time (t). Breakthrough and saturation time, biosorption yield (%), and Cr^{3+} uptake are relevant parameters that they can be obtained from the breakthrough curve as follows:

- Breakthrough time (t_b, min) is considered on the basis of the effluent discharge limit for Cr^{3+}. So, the breakthrough time was obtained for an effluent Cr^{3+} concentration of 5 mg/L.
- Saturation time (t_{sat}, min) is usually considered when the effluent concentration remains close to influent concentration for a long period.
- The uptake capacity (q_{ads}, mmol/g) is obtained by dividing the quantity of Cr^{3+} biosorbed (m_{ads}) by the sorbent mass (m).

$$q_{ads} = \frac{m_{ads}}{m} \tag{2}$$

where the total quantity of Cr^{3+} biosorbed in the column (m_{ads}, mmol) is calculated from the area above the breakthrough curve multiplied by the flow rate (Q, L/min).

$$m_{ads} = Q \cdot \int_0^{t_b} (C_0 - C) \cdot dt \tag{3}$$

- The Cr^{3+} biosorption yield (%) can be calculated as follows:

$$Cr^{3+}\ \text{biosorption yield} = \frac{m_{ads}}{m_{total}} \cdot 100 \tag{4}$$

where the total amount of Cr^{3+} (m_{total}, mmol) can be obtained as follows:

$$m_{total} = C_0 \cdot Q \cdot t_{sat} \tag{5}$$

Various simple mathematical models have been developed to describe and possibly predict the dynamic behaviour of the column bed. One of the most widely used models for the continuous flow conditions is the BDST model, which is a straightforward model for predicting the relationship between bed depth and service time in terms of process concentrations and biosorption parameters. The model is based on physically measuring the capacity of the bed at different breakthrough values. It ignores intraparticle mass transfer resistance and external film resistance, so that the sorbate is sorbed onto the biosorbent surface directly [41]. The rate of sorption is controlled by the surface reaction between sorbate and the unused capacity of the biosorbent.

The experimental breakthrough curves at two different bed heights and those obtained for the BDST model are represented in Fig. 7. The experimental breakthrough time (the position at C/C_0 = 0.25), saturation time (the position at C/C_0 = 0.99), biosorption yield (%) and Cr^{3+} uptake (mmol/g), as well as the BDST

Table 4
Different experimental parameters of the breakthrough curves and characteristic parameters of BDST model, along with the values of average relative errors (ARE, %) and coefficients of determination (r).

Test	Experimental values				BDST model			
	t_b (min)	t_{sat} (min)	% Ads	q_{ads} (mmol/g)	N_0 (mmol/L)	k_a (L/mmol h)	r	ARE (%)
H = 25.5 cm	1025	2922	49.4	0.24	40.4	0.66	0.99	6.9
H = 34 cm	1523	3426	57.5	0.24	42.7	0.54	0.99	6.9

parameters, the determination coefficient and the average relative error, are tabulated in Table 4. The concentration profiles of the solution exiting the column show that the adsorption zone, the part of the column where adsorbate is transferred to the adsorbent, continues increasing and finally coincides with the top of the column, the metal ion concentration gradually rising and approaching the feed concentration [42]. Chromium removal is fast and highly effective during the initial phase. Subsequently, metal removal decreases, as a consequence of the progressive saturation of the binding sites. As it can be seen, a displacement of the adsorption front with an increase in height was obtained. The breakthrough time, the saturation time and the biosorption yield increase as bed height increases since a higher bed depth results in a longer residence time of the solution in the column, allowing the metal ions to diffuse more deeply inside the biosorbent, and so, all the above parameters increase. For the two bed heights assayed, the effluent pH initially increased (up to 6) and then gradually decreased to reach the pH value of the influent (data not shown). This might be due to the release of light ions like Ca^{2+}, Mg^{2+}, Na^{+} and K^{+} present in the orange waste to the solution. In contrast and contrary to expected, the amounts of Cr^{3+} sorbed per unit of mass in the continuous assays were significantly lower than those obtained in batch assays. These findings agree with other published results [43,44] and suggest that lower contact time between adsorbate and adsorbent for column mode operation is one of the main reasons for such a decrease in uptake values. Due to the slow kinetics of chromium sorption onto orange waste, the metal ions do not have sufficient time to diffuse into the whole of the biosorbent mass in column mode operation, and so the amount of Cr^{3+} sorbed is considerably reduced.

The low value of the average relative error (ARE < 7%) and the high value of the correlation coefficient (r > 0.99) confirm the good fit of this model and infers that the BDST model successfully describes the breakthrough curves for the removal of Cr^{3+} by orange waste. The satisfactory fitting of the experimental data and the BDST modelled breakthrough curves confirm that the sorption mechanism could be controlled by chemical reaction.

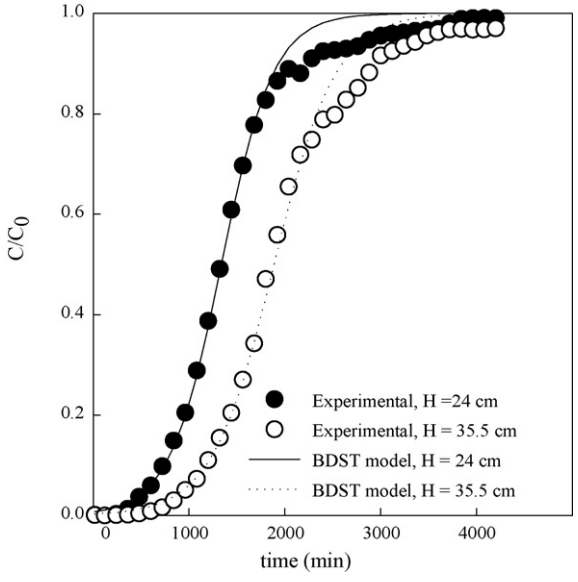

Fig. 7. Column breakthrough curves for adsorption of Cr^{3+} on orange waste beds.

4. Conclusions

In light of the experimental results obtained and their evaluation, orange waste, an agrobased waste material, has considerable potential for use in the removal of chromium from aqueous solutions.

FTIR analysis of the biosorbent, before and after chromium sorption, shows that carboxylic and hydroxyl groups could be the major functional groups involved in metal binding to the orange waste.

The metal uptake by biosorption is strongly affected by parameters such as adsorbent dosage and pH, whereas adsorbent particle size had no significant effect on Cr^{3+} uptake. The higher the adsorbent dose and pH, the higher the metal removal attained.

Kinetic studies show that chromium took approximately 3 days to reach equilibrium. Experimental data can be described adequately by a pseudo-second order kinetic, confirming the chemisorption of chromium onto orange waste.

The Sips and the Redlich–Peterson isotherm models were found to fit the equilibrium data well. The values obtained for maximum sorption capacity in this work are within the range described in previous studies.

Dynamic adsorption studies revealed that orange waste could be successfully used as biosorbent for treating effluents containing Cr (III) and breakthrough curves can be satisfactorily fitted to the BDST model.

Acknowledgement

The authors wish to express their gratitude to the Spanish Ministry of Science and Technology for the funding of this work.

References

[1] O.S. Amuda, A.A. Giwa, I.A. Bello, Removal of heavy metal from industrial wastewater using modified activated coconut shell carbon, Biochem. Eng. J. 36 (2007) 174–181.
[2] U.K. Garg, M.P. Kaur, V.K. Garg, D. Sud, Removal of hexavalent chromium from aqueous solution by agricultural waste biomass, J. Hazard. Mater. 140 (2007) 60–68.
[3] C. Quintelas, B. Fonseca, B. Silva, H. Figueiredo, T. Tavares, Treatment of chromium(VI) solutions in a pilot-scale bioreactor through a biofilm of *Arthrobacter viscosus* supported on GAC, Biores. Technol. 100 (1) (2009) 220–226.
[4] Y.S. Yun, D. Park, J.M. Park, B. Volesky, Biosorption of trivalent chromium on the brown seaweed biomass, Environ. Sci. Technol. 35 (2001) 4353–4358.
[5] B.J. Alloway, A.K. Ayres, Chemical Principles of Environmental Pollution, second ed., Blackie/Chapman and Hall, London/New York, 1997, p. 214.
[6] O.D. Uluozlu, A. Sari, M. Tuzen, M. Soylak, Biosorption of Pb(II) and Cr(III) from aqueous solution by lichen (*Parmelina tiliaceae*) biomass, Biores. Technol. 99 (8) (2008) 2972–2980.
[7] B. Volesky, Removal and recovery of heavy metals by biosorption, in: B. Volesky (Ed.), Biosorption of Heavy Metals, CRC Press, Boca Raton, 1990, pp. 7–44.
[8] M.C. Basso, E.G. Cerrella, A.L. Cukierman, Lignocellulosic materials as potential biosorbents of trace toxic metals from wastewater, Ind. Eng. Chem. Res. 41 (2002) 3580–3585.
[9] B. Nasernejad, T. Esslam Zadeh, B. Bonakdar Pour, M. Esmaail Bygi, A. Zamani, Comparison for biosorption modeling of heavy metals (Cr (III), Cu (II), Zn (II)) adsorption from wastewater by carrot residues, Process Biochem. 40 (3–4) (2005) 1319–1322.

[10] K. Chojnacka, Biosorption of Cr(III) ions by eggshells, J. Hazard. Mater. 121 (1–3) (2005) 167–217.
[11] H. Parab, S. Joshi, N. Shenoy, A. Lali, U.S. Sarma, M. Sudersanan, Determination of kinetic and equilibrium parameters of the batch adsorption of Co(II), Cr(III) and Ni(II) onto coir pith, Process Biochem. 41 (3) (2006) 609–615.
[12] L.H. Wang, C.I. Lin, Adsorption of chromium (III) ion from aqueous solution using rice hull ash, J. Chin. Inst. Chem. Eng. 39 (4) (2008) 367–373.
[13] G. Blázquez, F. Hernáinz, M. Calero, M.A. Martín-Lara, G. Tenorio, The effect of pH on the biosorption of Cr (III) and Cr (VI) with olive stone, Chem. Eng. J. 148 (2–3) (2008) 473–479.
[14] N. Feng, X. Guo, S. Liang, Adsorption study of copper (II) by chemically modified orange peel, J. Hazard. Mater. 164 (2–3) (2009) 1286–1292.
[15] C. Namasivayam, I.R. Kavitha, XRD and SEM studies on the mechanism of adsorption of dyes and phenols by coir pith carbon from aqueous phase, Microchem. J. 82 (2006) 43–48.
[16] C. Bouchelta, M.S. Medjram, O. Bertrand, J.P. Bellat, Preparation and characterization of activated carbon from date stones by physical activation with steam, J. Anal. Appl. Pyrolysis 82 (1) (2008) 70–77.
[17] H. Arslanoglu, H.S. Altundogan, F. Tumen, Preparation of cation exchanger from lemon and sorption of divalent heavy metals, Biores. Technol. 99 (7) (2008) 2699–2705.
[18] A. Sari, D. Mendil, M. Tuzen, M. Soylak, Biosorption of Cd(II) and Cr(III) from aqueous solution by moss (*Hylocomium splendens*) biomass: equilibrium, kinetic and thermodynamic studies, Chem. Eng. J. 144 (1) (2008) 1–9.
[19] P. Lodeiro, A. Fuentes, R. Herrero, M.E.S. de Vicente, Cr(III) binding by surface polymers in natural biomass: the role of carboxylic groups, Environ. Chem. 5 (2008) 355–365.
[20] A.B. Pérez Marín, J.F. Ortuño, M.I. Aguilar, V.F. Meseguer, J. Sáez, M. Lloréns, Use of chemical modification to determine the binding of Cd(II), Zn(II) and Cr(III) ions by orange waste, Biochem. Eng. J. (2009), doi:10.1016/j.bej.2008.12.010.
[21] J.C.P. Vaghetti, E.C. Lima, B. Royer, B.M. da Cunha, N.F. Cardoso, J.L. Brasil, S.L.P. Dias, Pecan nutshell as biosorbent to remove Cu(II), Mn(II) and Pb(II) from aqueous solutions, J. Hazard. Mater. 162 (1) (2009) 270–280.
[22] A.H. Ören, A. Kaya, Factors affecting adsorption characteristics of Zn^{2+} on two natural zeolites, J. Hazard. Mater. 131 (1–3) (2006) 59–65.
[23] G. Blázquez, F. Hernáinz, M. Calero, L.F. Ruiz-Núñez, Removal of cadmium ions with olive stones: the effect of somes parameters, Process Biochem. 40 (8) (2005) 649–2654.
[24] C.E. Dogan, K. Turhan, G. Akcin, A. Aslan, Biosorption of Au (III) and Cu (II) from aqueous solution by a non-living *Cetraria islandica* (*L.*) Ach, Ann. Chim. 96 (3–4) (2006) 229–236.
[25] Z.V.P. Shaik Basha, B.Jha. Murthy, Sorption of Hg(II) onto *Carica papaya*: experimental studies and design of batch sorber, Chem. Eng. J. 147 (2–3) (2008) 226–234.
[26] S. Al-Asheh, F. Banat, R. Al-Omari, Z. Duvnjak, Predictions of binary adsorption isotherms for the adsorption of heavy metals by pine bark using single isotherm data, Chemosphere 41 (2000) 659–665.
[27] R.L. Ramos, L.F. Rubio, R.M.G. Coronado, J.M. Barron, Adsorption of trivalent chromium from aqueous solutions onto activated carbon, J. Chem. Technol. Biotechnol. 12 (1995) 64–67.
[28] J. Rivera-Utrilla, M. Sánchez-Polo, F. Carrasco-Marín, Adsorption of 1,3,6-naphthalenetrisulfonic acid on activated carbon in the presence of Cd(II), Cr(III), and Hg(II). Importance of electrostatic interactions, Langmuir 19 (2003) 10857–10861.
[29] M. Ajmal, R.A.K. Rao, R. Ahmad, J. Ahmad, Adsorption studies on *Citrus reticulata*: removal and recovery of Ni(II) from electroplating wastewater, J. Hazard. Mater. B79 (2000) 117–131.
[30] G. Annadurai, R.-S. Juang, D.-J. Lee, Use of cellulose-based wastes for adsorption of dyes from aqueous solutions, J. Hazard. Mater. 92 (3) (2002) 263–274.
[31] S.H. Lee, C.H. Jung, H.M. Chung, Y. Lee, J.-W. Yang, Removal of heavy metals from aqueous solution by apple residues, Process Biochem. 33 (1998) 205–211.
[32] C.W. Cheung, J.F. Porter, G. McKay, Elovich equation and modified second-order equation for adsorption of cadmium ions onto bone char, J. Chem. Technol. Biotechnol. 75 (11) (2000) 963–970.
[33] Y.S. Ho, G. McKay, Sorption of lead (II) ions on peat, Water Res. 33 (2) (1999) 578–584.
[34] Y. Bulut, Z. Tez, Adsorption studies on ground shells of hazelnut and almond, J. Hazard. Mater. 149 (1) (2007) 35–41.
[35] M. Özacar, I.A. Sengil, A kinetic study of metal complex dye adsorption onto pine sawdust, Process Biochem. 40 (2005) 565–572.
[36] R.S. Juang, M.L. Chen, Application of the Elovich equation to the kinetics of metal sorption with solvent-impregnated resins, Ind. Eng. Chem. Res. 36 (1997) 813–820.
[37] C.W. Cheung, J.F. Porter, G. McKay, Sorption kinetic analysis for the removal of cadmium ions from effluents using bone char, Water Res. 35 (3) (2001) 605–612.
[38] J.C.P. Vaghetti, E.C. Lima, B. Royer, J.L. Brasil, B.M. da Cunha, N.M. Simon, N.F. Cardoso, C.P. Zapata Noreña, Application of Brazilian-pine fruit coat as a biosorbent to removal of Cr(VI) from aqueous solution-kinetics and equilibrium study, Biochem. Eng. J. 42 (1) (2008) 67–76.
[39] F. Gimbert, N.M. Crini, F. Renault, P.M. Badot, G. Crini, Adsorption isotherm models for dye removal by cationized starch-based material in a single component system: error analysis, J. Hazard. Mater. 157 (1) (2008) 34–46.
[40] A.R. Iftikhar, H.N. Bhatti, M.A. Hanif, R. Nadeem, Kinetic and thermodynamic aspects of Cu(II) and Cr(III) removal from aqueous solutions using rose waste biomass, J. Hazard. Mater. 161 (2–3) (2009) 941–947.
[41] P.A. Kumar, S. Chakraborty, Fixed-bed column study for hexavalent chromium removal and recovery by short-chain polyaniline synthesized on jute fiber, J. Hazard. Mater. 162 (2–3) (2009) 1086–1098.
[42] N. Sharma, K. Kaur, S. Kaur, Kinetic and equilibrium studies on the removal of Cd^{2+} ions from water using polyacrylamide grafted rice (*Oryza sativa*) husk and (*Tectona grandis*) saw dust, J. Hazard. Mater. 163 (2009) 1338–1344.
[43] Z. Aksu, F. Gönen, Z. Demircan, Biosorption of chromium(VI) ions by Mowital® B30H resin immobilized activated sludge in a packed bed: comparison with granular activated carbon, Process Biochem. 38 (2002) 175–186.
[44] V.C. Taty-Costodes, H. Fraduet, C. Porte, Y.S. Ho, Removal of lead(II) ions from synthetic and real effluents using immobilized *Pinus sylvestris* sawdust: adsorption on a fixed-bed column, J. Hazard. Mater. B123 (2005) 135–144.